

Magnetic Phases in Periodically Rippled Graphene.

M. Pilar López-Sancho and Luis Brey*

*Departamento de Teoría y Simulación de Materiales,
Instituto de Ciencia de Materiales de Madrid, CSIC, 28049 Cantoblanco, Spain*

(Dated: August 22, 2021)

We study the effects that ripples induce on the electrical and magnetic properties of graphene. The variation of the interatomic distance created by the ripples translates in a modulation of the hopping parameter between carbon atoms. A tight binding Hamiltonian including a Hubbard interaction term is solved self consistently for ripples with different amplitudes and periods. We find that, for values of the Hubbard interaction U above a critical value U_C , the system displays a superposition of local ferromagnetic and antiferromagnetic ordered states. Nonetheless the global ferromagnetic order parameter is zero. The U_C depends only on the product of the period and hopping amplitude modulation. When the Hubbard interaction is close to the critical value of the antiferromagnetic transition in pristine graphene, the antiferromagnetic order parameter becomes much larger than the ferromagnetic one, being the ground state similar to that of flat graphene.

I. INTRODUCTION

Graphene is a two-dimensional material with many possibilities in technological applications[1, 2], but also it presents many exotic and unexpected physical peculiarities[3, 4]. One of the more remarkable new physical properties of graphene is the strain-induced pseudo magnetic gauge fields[5, 6]. In graphene uniform strain, apart from a renormalization of the Dirac velocity, generates a constant gauge vector potential that shift the position in reciprocal space of the Dirac cones and can be gauged away. On the contrary non-uniform strain generates position dependent vector potential that induces pseudo-magnetic fields which can be experimentally tested. Non-uniform strain occurs in the intrinsic ripples that appear in free standing graphene[7–10] and also when the graphene sheet is bonded to a substrate[11–16]. Effective magnetic fields constant on large areas can be obtained by strain engineering[17–22]. The effective fields generated by non uniform strain can interfere with externally applied magnetic fields giving rise to new physical effects[23–25]. Also the existence of pseudo magnetic fields could produce anomalous effects in the electronic quantum transport[26].

The origin of the appearance of the gauge fields is the lineal dispersion of the bands near the Dirac points[27] and gauge fields have been predicted to occur in a variety of physical systems with linear dispersion as topological insulators[28, 29], optical lattices[30], modulated graphene superlattice[31], molecular graphene[32] and other two-dimensional semimetals[33].

Previous work has shown that the application of an uniform uniaxial strain to graphene reduces the value of the critical coupling constant for exchange instability towards a ferromagnetic (FM) phase[34, 35]. Also, the critical value of the on-site Hubbard coupling for an antiferromagnetic (AFM) instability was found to be reduced

with respect the case of pristine graphene[36–38]. In the case of non uniform strain the appearance of pseudo magnetic fields induces a peak in the density of states at the Fermi energy and the instability of the system against magnetic ordering. In this work we study, by solving self-consistently the Hubbard model, the electrical and magnetic properties of rippled graphene. We model the graphene ripple, a lattice deformation, by a sinusoidal modulation of the hopping parameter of period L and amplitude δ_t .

The main results of our work are summarized in Fig.1 and Fig.2. In rippled graphene, for non-interacting electrons, eight degenerated pseudo Landau levels appear at the Fermi energy, see Fig.1(a), from which only half will be occupied. For values of the Hubbard interaction greater than a critical U_C , the high density of states at the Fermi energy makes the system magnetically unstable and the minimization of the exchange energy opens an energy gap and selects the four occupied pseudo Landau levels. We obtain numerically that U_C depends only on the product of the ripple amplitude by its period $\delta_t L$, as shown in Fig.2. For small values of this parameter U_C coincides practically with the critical value of the paramagnetic antiferromagnetic transition in pristine graphene, U_C^{AF} . For larger values of the product $\delta_t L$ the value of U_C decreases until it reaches zero.

For values of U slightly higher than U_C the system presents a local ferromagnetic order that correlates its polarization with the orientation of the pseudo magnetic field, Fig.1(b), in such a way that the total magnetization is zero. On top of the local FM order there is an antiferromagnetic order with a small order parameter. For larger values of U the pseudo Landau levels are destroyed and the antiferromagnetic order parameter increases being much larger than the local FM order parameters, as schematically shown in Fig.1(c).

Our results are consistent with the obtained in reference [21], where a strained graphene flake is studied with an almost uniform axial pseudo magnetic field in the bulk that is compensated by an opposite oriented pseudo magnetic field at the edge. In this geometry, on top of a global

* Electronic address: brey@icmm.csic.es

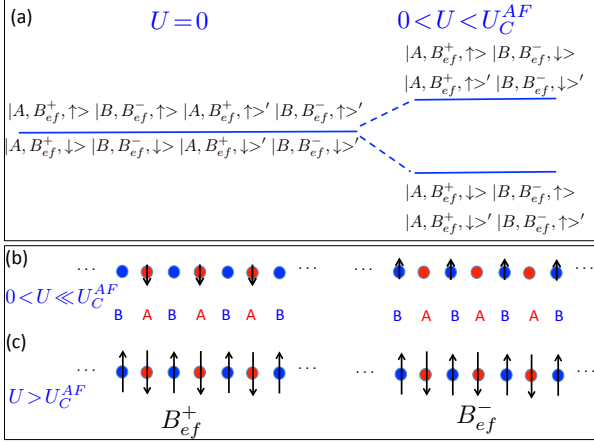


FIG. 1. (Color online) (a) Pseudo Landau levels appearing in rippled graphene. In absence of interactions, $U = 0$, there are eight zero energy degenerated pseudo Landau levels corresponding to states located in regions with positive, B_{ef}^+ , or negative, B_{ef}^- effective magnetic fields, with spin projection \uparrow or \downarrow , and in Dirac points \mathbf{K} or \mathbf{K}' . In regions with $B_{ef}^{+(-)}$ the wave functions have only amplitude in sublattice $A(B)$. A moderate interaction U opens an exchange energy gap, favoring a local FM order in regions with B_{ef}^+ and opposite polarized FM order in regions with B_{ef}^- . In (b) we show schematically the real space magnetic order for moderate U . For larger values of the Hubbard interaction (c), rippled graphene gets a Néel order with a very weak FM modulation.

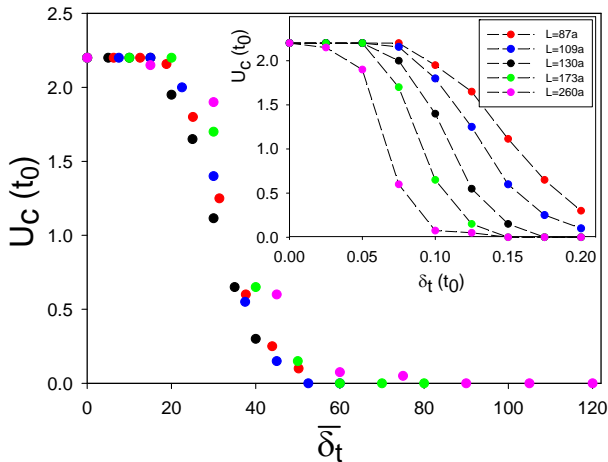


FIG. 2. (Color online) Critical Hubbard interaction for magnetic instabilities in rippled graphene, as function of the dimensionless parameter $\bar{\delta}_t = \frac{\delta_t}{\hbar v_F G}$. Dots with different colors correspond to different values of the period L . In the inset we plot U_C as function of δ_t and for different periods L .

AFM order, the bulk and the edge of the flake have an effective but opposite oriented magnetization[21].

The paper is organized as follows. In the next section we introduce the ripple geometry and the tight-binding and Dirac like Hamiltonians describing the electronic properties of the system. Also we refresh the concept of gauge magnetic field. In section III, we obtain, by perturbation theory, the low energy states of graphene with a sinusoidal modulation of the hopping and identify the eight zero energy Landau levels that appear in rippled graphene. Section IV is devoted to the study of the effect of the electron-electron interaction on the electronic properties. We also present self-consistent results obtained from the Hubbard Hamiltonian. Finally, the results are summarized in section V.

II. GEOMETRY AND HAMILTONIAN

Geometry. In graphene the carbon atoms crystallize in a two-dimensional triangular lattice with a basis constituted by two equivalent atoms A and B . The lattice is defined, see Fig.3, by the vectors $\mathbf{a} = \frac{a}{2}(\sqrt{3}, 1)$ and $\mathbf{b} = \frac{a}{2}(\sqrt{3}, -1)$, and the atoms of the basis are located at the origin, $(0, 0)$ and at $\delta = (a/\sqrt{3}, 0)$, here $a = 2.46\text{\AA}$ is the lattice parameter. As discussed in the introduction, the ultrathin nature of graphene makes it flexible against out-of-plane deformations of the lattice. Here, we consider a one-dimensional periodic graphene ripple, which modulates the height (z -coordinate) of the carbon atoms according to the expression

$$h(x) = h_0 \sin \frac{\pi}{L} x \quad (1)$$

where $\mathbf{r} = (x, y)$ is the position of the carbon atoms, h_0 is the height amplitude and the period is $L/2$, as schematically shown in Fig.3.

Tight-Binding Hamiltonian. The electronic properties of graphene are well described by a nearest neighbor tight-binding Hamiltonian[3, 4] of the form

$$H_0 = - \sum_{\langle i,j \rangle, \sigma} \left(t_{i,j} c_{i,\sigma,A}^\dagger c_{j,\sigma,B} + h.c \right), \quad (2)$$

where $c_{i,\sigma,\alpha}^\dagger$ creates an electron at lattice site i with spin σ and sublattice $\alpha = A, B$.

In pristine graphene the distance between first neighbor carbon atoms is the same along the entire crystal and the hopping between atoms is constant $t_{i,j} = t_0$, with $t_0 = 2.8eV$. In rippled graphene the corrugation modifies the distance between carbon atoms. When the period of the ripple is much larger than a , the distance between two first neighbor carbon atoms i and j located at \mathbf{r}_i and \mathbf{r}_j is modified to

$$d_{i,j} \approx d_0 \left(1 + \frac{\pi^2}{2} \frac{h_0^2}{L^2} \frac{(x_j - x_i)^2}{d_0^2} \cos^2 \frac{\pi}{L} x_i \right) \quad (3)$$

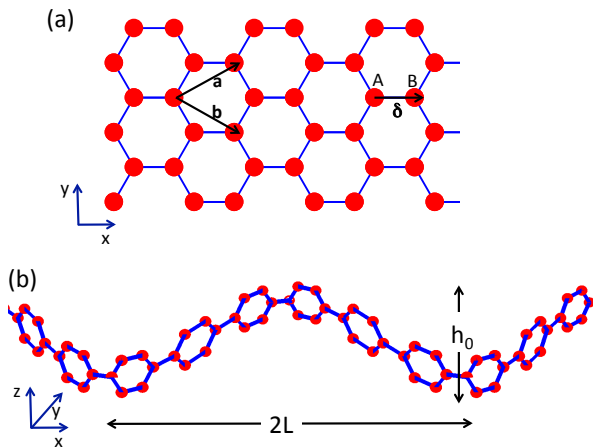


FIG. 3. (Color online) (a) Graphene crystal structure, **a** and **b** indicated the lattice vectors. δ is the vector connecting the two atoms, A and B, in the unit cell. (b) Schematic view of a graphene ripple of period $2L$ and height h_0 .

being $d_0 = a/\sqrt{3}$ the equilibrium distance between carbon atoms.

The hopping amplitude between nearest neighbor atoms scales with a power law with the length of the bond between atomic centers[39–41],

$$t_{i,j} = t_0 \left(\frac{d_0}{d_{i,j}} \right)^\beta \approx t_0 \left(1 - \frac{\beta\pi^2 h_0^2 (x_j - x_i)^2}{2 L^2 d_0^2} \cos^2 \frac{\pi}{L} x_i \right) \quad (4)$$

being $\beta \sim 2 - 3$. Therefore, a ripple with period $L/2$ induces a modulation in the hopping amplitude with period L . The modulation of the hopping is proportional to $\sim 10 \frac{h_0^2}{L^2}$, that for some experimental systems can be as larger as 0.1[9].

Dirac Hamiltonian. The low energy, long distance electronic excitations of graphene occur near the celebrated Dirac points, $\mathbf{K} = \frac{2\pi}{a} (\frac{1}{\sqrt{3}}, \frac{1}{3})$ and $\mathbf{K}' = \frac{2\pi}{a} (\frac{1}{\sqrt{3}}, -\frac{1}{3})$. Near these points, the band structure of graphene is very well described by Dirac-like Hamiltonians,

$$H_D = \hbar v_F (i s \partial_y \tau_x - i \tau_y \partial_x) \quad (5)$$

where $v_F = \frac{\sqrt{3}}{2} t_0 a$, and $\boldsymbol{\tau} = (\tau_x, \tau_y, \tau_z)$ are the Pauli matrices acting on a spinor that define the amplitude of the wave function on the sublattices A and B of graphene and $s = +1$ and $s = -1$ indicates the Dirac cone \mathbf{K} and \mathbf{K}' respectively. In presence of a hopping modulation of the form of equation 4, the modified Dirac Hamiltonians take the form [8],

$$H_D = \hbar \bar{v}_F(x) (i s \partial_y \tau_x - i \tau_y \partial_x) + (t_{\parallel}(x) - t_{\perp}(x)) \tau_x \quad (6)$$

where $t_{\parallel}(x)$ and $t_{\perp}(x)$ are the hopping parameters corresponding to the horizontal and oblique bonds, see Fig.3 and $\bar{v}_F(x) = \frac{\sqrt{3}}{2} a t_{\perp}(x)$. We assume that the period of the

ripple is much larger than the graphene lattice parameter and electronic states coming from different Dirac cones do not mix. The modulation of the hopping has two effects on the electronic properties of graphene, it modulates spatially the Fermi velocity and creates a position dependent gauge magnetic field[8, 27, 42–44].

Magnetic gauge field. In this work we are interested on the effect of the gauge field on the graphene electronic properties, therefore in order to avoid effects related with the modulation of the Fermi velocity, we only consider modification in the horizontal hoping t_{\parallel} and we take $t_{\perp} = t_0$ and the Dirac Hamiltonian takes the form[45]

$$H_D(\mathbf{r}) = \hbar v_F (i s \partial_y \tau_x - i \tau_y \partial_x) + \delta_t \sin Gx \tau_x \quad (7)$$

with $G = 2\pi/L$ and $\delta_t = \frac{\beta\pi^2}{4} \frac{h_0^2}{L^2} t_0$.

With this assumption the modulation of the hopping results in the appearance of the vector potential $A_y = s \frac{c\delta_t}{e v_F} \sin Gx$. The vector potential has opposite sign in different Dirac points, so that time reversal symmetry is preserved. For a given Dirac cone, the effective vector potential oscillates in space forming alternating regions of positive and negative pseudo magnetic fields, $B_z = s \frac{c\delta_t}{e v_F} G \cos Gx$. The magnetic length corresponding to the maximum of the pseudo magnetic field is $\ell = \sqrt{\frac{\hbar v_F}{\delta_t G}}$. A wave function in the $n = 0$ pseudo Landau level should be localized in the region where the pseudo magnetic field has a defined sign, i.e. $\ell < L/2$. That implies that, for observing physical effects related with the pseudo Landau levels quantization, the parameters describing the ripple should satisfy,

$$\frac{2\hbar v_F}{\pi L \delta_t} < 1 \quad \text{or equivalently} \quad \frac{4\sqrt{3} La}{\beta\pi^3 \hbar_0^2} < 1 \quad . \quad (8)$$

For values $\delta_t \sim 0.05t_0 - 0.1t_0$ and a period of the hopping modulation $L = 200a$, the effective magnetic length takes values in the interval $40a - 56a$, smaller than $L/2$, that correspond to effective magnetic fields in the range of 27T-38T.

Symmetry Considerations. We are interested in obtaining the energy spectrum of the system as function of the momentum \mathbf{k} , that in the following we define with respect to the Dirac points. We begin by considering some symmetries of graphene in presence of a ripple. We have already mentioned that because the gauge magnetic fields have opposite sign on opposite Dirac points, time reversal symmetry is preserved. On the other hand the Hamiltonian does not depend on the coordinate y , and therefore the momentum k_y is a good quantum number and the eigenfunction can be written as $\varphi_{k_y}(\mathbf{r}) = \psi_{k_y}(x) e^{i k_y y}$, where $\psi_{k_y}(x)$ is an eigenfunction of the effective Hamiltonian $H_D(x, k_y) = e^{-i k_y y} H_D(\mathbf{r}) e^{i k_y y}$. Besides, the low energy Dirac Hamiltonian, Eq.7 satisfies the relation $\tau_z H_D(x) \tau_z = -H_D(x)$, and this implies that for any eigenstate with momentum \mathbf{k} and energy $E(\mathbf{k})$ there is a state with opposite energy and the same momentum. Finally, the Hamiltonian has the property

$H_D(-k_y, x + L/2) = \tau_z H_D^*(k_y, x) \tau_z$ that implies that for any zero energy state appearing at a particular k_y , there exists another zero mode at momentum $-k_y$.

III. PERTURBATION THEORY.

The low energy Hamiltonian, Eq.7, when $k_y=0$ presents zero energy states with the explicit form, $\psi_{k_y=0}^1 = (e^{\bar{\delta}_t \cos Gx}, 0)^\dagger$ and $\psi_{k_y=0}^2 = (0, e^{-\bar{\delta}_t \cos Gx})^\dagger$ that for small values of the magnetic length ℓ take the form of gaussians centered at $x=nL$ and $x=L/2+nL$ respectively and have amplitude just in one of the graphene sublattices, here n is an integer and $\bar{\delta}_t = \frac{\delta_t}{\hbar v_F G}$. For finite values of k_y it is not possible to obtain analytical solutions, but we expect the wavefunctions $\psi_{k_y}^1$ and $\psi_{k_y}^2$ to be centered at $x=sk_y\ell^2$ and $x=L/2-sk_y\ell^2$ respectively. Therefore for small values of k_y we choose the basis

$$\begin{aligned} \psi_{k_y}^1 &= \frac{1}{\sqrt{I_0(2\bar{\delta}_t)}} \begin{pmatrix} e^{\bar{\delta}_t \cos G(x-sk_y\ell^2)} \\ 0 \end{pmatrix} \\ \psi_{k_y}^2 &= \frac{1}{\sqrt{I_0(2\bar{\delta}_t)}} \begin{pmatrix} 0 \\ e^{-\bar{\delta}_t \cos G(x+sk_y\ell^2)} \end{pmatrix} \end{aligned} \quad (9)$$

where I_0 is the modified Bessel function of the first kind of zero-order. For small wave vector the wavefunctions ψ_1 and ψ_2 are similar to the zero energy real magnetic field Landau levels [46]. However the structure of the spinors is different. For the valley \mathbf{K} the wavefunction $\psi_{k_y}^1$ has only amplitude in sublattice A and it is centered at positions near $x = nL$, where the pseudo magnetic field is positive, B_{ef}^+ , on the contrary $\psi_{k_y}^2$ has only support in sublattice B and is located in the regions near $x=nL + L/2$ where the effective magnetic field is negative, B_{ef}^- . For the Dirac cone \mathbf{K}' , the spatial locations of the wavefunctions $\psi_{k_y}^1$ and $\psi_{k_y}^2$ are reversed with respect the \mathbf{K} valley, so that time reversal symmetry is preserved.

The Hamiltonian of Eq.7 projected in the basis given by Eq.9 takes the form,

$$\bar{H} = \begin{pmatrix} 0 & t(k_y) \\ t(k_y) & 0 \end{pmatrix} \quad (10)$$

with

$$t(k_y) = \frac{-\hbar v_F k_y \bar{I}_0 + \delta_t \bar{I}_1 (1 - \cos(Gk_y \ell^2)) \text{sgn}(k_y)}{I_0(2\bar{\delta}_t)} \quad (11)$$

where $\bar{I}_n = I_n(\bar{\delta}_t \sin(Gk_y \ell^2))$ being I_n the modified Bessel function of the first kind of order n . At small momenta k_y the dispersion is lineal with renormalized velocity

$$\bar{v}_F = v_F / I_0(2\bar{\delta}_t), \quad (12)$$

which, although finite, decreases exponentially when increasing L or δ_t . As a result of that, the band structure obtained in numerical calculations [8, 47] shows apparent dispersionless degenerate pseudo Landau levels. For

larger values of k_y the overlap between the wavefunctions $\psi_{k_y}^1$ and $\psi_{k_y}^2$ increases and the pseudo Landau levels acquire a dispersion. Therefore, at zero energy, there are eight almost degenerated pseudo Landau levels, Fig.1, denoted by $|A, B_{ef}^+, \sigma \rangle$, $|B, B_{ef}^-, \sigma \rangle$, $|A, B_{ef}^+, \sigma \rangle'$ and $|B, B_{ef}^-, \sigma \rangle'$, in such a way that in regions with $B_{ef}^{+(-)}$ the states have amplitude only in sublattice $A(B)$. Here σ is the projection of the electron spin.

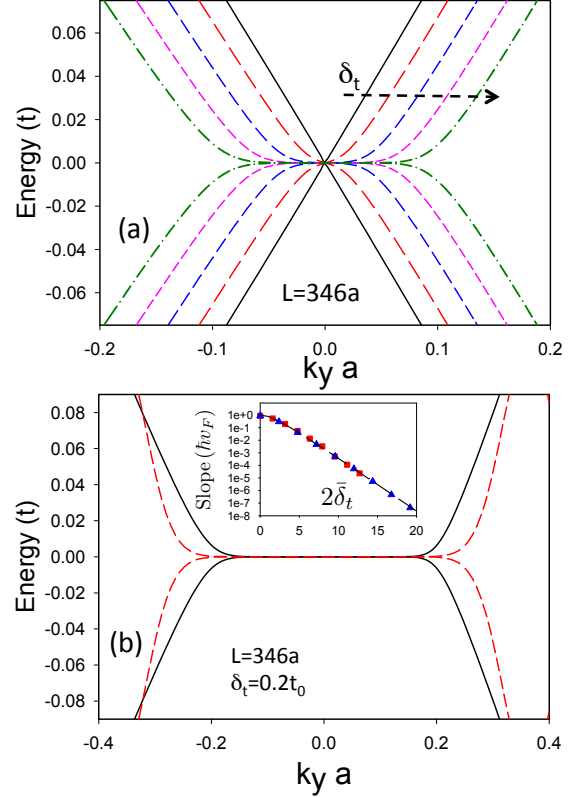


FIG. 4. (Color online) (a) Band structure near a Dirac point for graphene in presence of a sinusoidal modulation of the hopping with period $L=246a$ and δ_t running from 0 to 0.1t. (b) same as (a) for $L = 346a$ and $\delta_t=0.2t$. Continuous lines correspond to tight binding results whereas dashed lines are the dispersion obtained using Eq.10. Inset in (b) shows, as function of the dimensionless parameter $\bar{\delta}_t$, the renormalized Fermi velocity at Dirac points for $L = 178a$ (triangles) and $L = 115a$ (squares) and values of δ_t ranging from zero to $\delta_t = 0.2t$. The dashed line corresponds to expression Eq.12.

Tight Binding results. In order to check the results obtained with the modified Dirac equations, we have performed microscopic tight binding calculations. We have considered a sinusoidal modulation of the hopping in a supercell along the x -direction with the geometry presented in Fig.3. In this geometry the Brillouin zone of the supercell is rectangular; in the y -direction goes from 0 to $\frac{2\pi}{a}$ and in the x direction from 0 to $\frac{2\pi}{L}$. For large values of L , the eigenvalues do not depend on k_x and we just consider $k_x = 0$. In this geometry the original Dirac

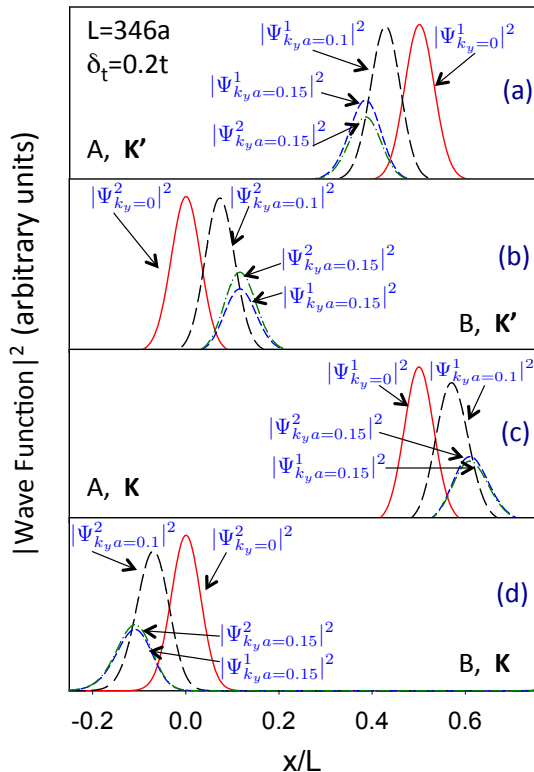


FIG. 5. (Color online) Square of the wavefunctions obtained from the tight binding calculation for wavevectors near the \mathbf{K}' (a-b) and \mathbf{K} (c-d) points. The momentum k_y is measured with respect the Dirac points. For each k_y we consider the two states, 1 and 2 closest to zero energy. Panels (a) and (c) correspond to the amplitude on sublattice A whereas panels (b) and (d) correspond to amplitude on sublattice B . The results are obtained in the tight-binding approximation with a sinusoidal modulation of the hopping of period $L=346a$ and amplitude $\delta_t=0.2t$.

points \mathbf{K}' and \mathbf{K} are folded at the wavevectors $(\frac{2\pi}{3a}, 0)$ and $(\frac{4\pi}{3a}, 0)$ respectively. As pointed out above, in order to avoid effects related with the spatial dependence of the Dirac velocity, we only modulate the hopping in the horizontal bonds. In Fig.4(a) we plot the lowest energy conduction band and the highest energy valence band of rippled graphene for a period modulation $L = 346a$ and different values of the amplitude modulation δ_t . As predicted by the Dirac equation the linear dispersion becomes flatter as δ_t increases and, for moderate values of the modulation, the dispersion reminds that of Landau levels. In the inset of Fig.4(b) we plot the slope of the dispersion at $k_y \rightarrow 0$ as function of the dimensionless parameter $2\delta_t$, for two different values of the period, $L = 178a$ and $L = 115a$ and different values of δ_t . In agreement with the continuous solution, we obtain that the velocity only depends on the the combination $\delta_t L$ and is determined with a high precision by the renormalized velocity given in Eq.12. In Fig.4(b) we compare

the band structure for a hopping modulation of period $L=346a$ and amplitude $\delta_t=0.2t$, as obtained from the tight-binding approximation and from the approximated solution of the Dirac equation, Eq.10. The perturbation solution describes qualitatively the almost dispersionless states that occur near the Dirac points for small wavevectors, where the overlap between the wavefunctions from Eq.9 is practically null and how, for large enough values of k_y , the basis wave functions overlap and the coupling between states induces a bonding-antibonding splitting. The trial wavefunctions given in Eq.9, for small wave vectors, qualitatively describe the solutions of the tight-binding Hamiltonian. In Fig.5 (a)-(b) we plot, for wavevectors near \mathbf{K}' the square of the wavefunction on sublattice A and B respectively. For small values of k_y the almost degenerated gaussian-like wave functions are located at $x=sk_y\ell^2$ and $x=L/2 - sk_y\ell^2$ and have amplitude only in sublattices A and B respectively. As the wave vector k_y increases the coupling between the wavefunctions increases, the energies of the states split and the states get amplitude on both sublattices. Fig.5 (c)-(d) represent the same as (a)-(b) respectively, for wavevectors near \mathbf{K} .

IV. ELECTRON-ELECTRON INTERACTION.

In this section we address the effects of electron-electron interactions on the zero energy pseudo Landau levels formed in graphene by the modulation of the hopping terms. For large values of the product $L\delta_t$, the high density of states at the Fermi energy implies instabilities of the system again broken symmetry states that open gaps at the Fermi energy. In the Dirac approximation of graphene, the valley and spin variables are equivalent isospin indices and ignoring small symmetry breaking terms due to lattice effects[48–50] and neglecting the difference between the inter and intra valley electro-electron interaction, the Hamiltonian is $SU(4)$ invariant. Therefore, in the framework of the quantum Hall ferromagnetism[51–53], we expect the ground state to break spontaneously the $SU(4)$ symmetry putting many electrons into the same pseudospin state and minimizing their exchange energy to the lowest value satisfying the Pauli exclusion principle[54–61] and opening an energy gap in the charge excitations.

These quantum Hall pseudoferrromagnetic ground states are degenerated and broken symmetry terms, lattice effects or Landau level mixing can lift the degeneracy favoring some particular isospin order. In the presence of a real magnetic field, mean field calculations using a tight-binding Hamiltonian with a Hubbard term obtain a real spin antiferromagnetic ground state[60] and, calculations using the Dirac equation including isospin anisotropy[62] predict as well an antiferromagnetic order[63].

We study here the electronic and magnetic properties of rippled graphene by obtaining self-consistently the

tight-binding Hamiltonian describing a sinusoidal modulation of the hopping in the x -direction (see Fig.3) with an on-site Hubbard interaction term of the form,

$$H_U = U \sum_{i,\alpha} n_{i,\uparrow,\alpha} n_{i,\downarrow,\alpha} \quad (13)$$

where $n_{i,\sigma,\alpha} = c_{i,\sigma,\alpha}^\dagger c_{i,\sigma,\alpha}$ is the fermionic number operator for lattice site i , spin projection $\sigma = \uparrow, \downarrow$ and sublattice α . The usual mean field decomposition of the on-site interaction leads to an effective one-particle interaction term,

$$H_U = U \sum_{i,\alpha} (\langle n_{i,\uparrow,\alpha} \rangle n_{i,\downarrow,\alpha} + \langle n_{i,\downarrow,\alpha} \rangle n_{i,\uparrow,\alpha} - \langle n_{i,\uparrow,\alpha} \rangle \langle n_{i,\downarrow,\alpha} \rangle) \quad (14)$$

$\langle n_{i,\sigma,\alpha} \rangle$ denotes the average occupation operators, that are obtained by solving self consistently the tight-binding Hamiltonian and the mean field Hubbard term. The nature of the self-consistent ground state is characterized by the following order parameters,

$$M_i = \langle n_{i,\uparrow,A} \rangle + \langle n_{i,\uparrow,B} \rangle - \langle n_{i,\downarrow,A} \rangle - \langle n_{i,\downarrow,B} \rangle$$

$$m_i = \langle n_{i,\uparrow,A} \rangle - \langle n_{i,\uparrow,B} \rangle - \langle n_{i,\downarrow,A} \rangle + \langle n_{i,\downarrow,B} \rangle, \quad (15)$$

which indicate the local ferromagnetic and antiferromagnetic order respectively.

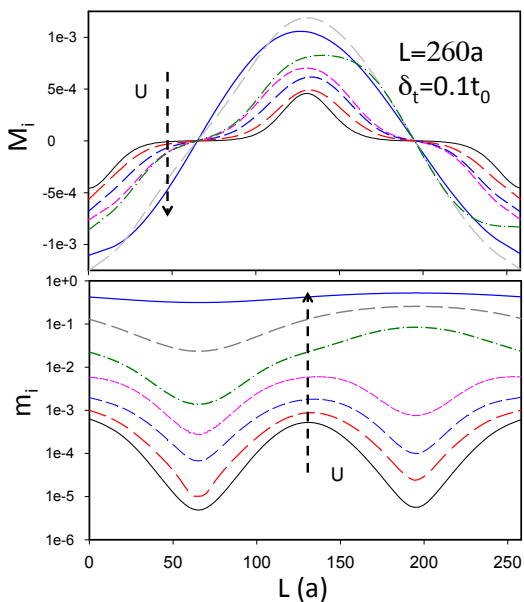


FIG. 6. (Color online) Ferromagnetic (top) and antiferromagnetic (bottom) local order parameter for a ripple with $\delta_t = 0.1t_0$, $L = 260a$ and $U = 0.5t_0, t_0, 1.5t_0, 2t_0, 2.2t_0, 2.3t_0$ and $2.5t_0$.

We have performed self-consistent calculations for different values of U , L , and δ_t . In all the cases we find that the charge is uniformly distributed, i.e. $\langle n_{i,\uparrow,A} \rangle +$

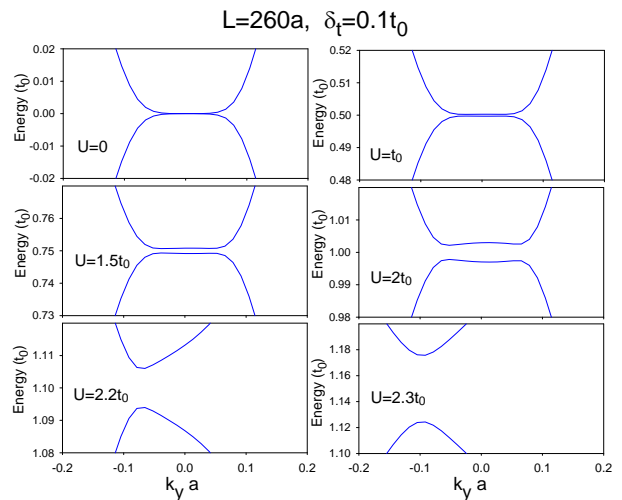


FIG. 7. (Color online) Band structure near Dirac point for graphene in presence of a sinusoidal modulation of the hopping with period $L = 246a$, $\delta_t = 0.1t_0$ and different values of the Hubbard coupling. The bands are spin degenerated.

$\langle n_{i,\downarrow,A} \rangle = \langle n_{i,\uparrow,B} \rangle + \langle n_{i,\downarrow,B} \rangle = 1$. For a given ripple characterized by a period L and a hopping modulation δ_t , there is a critical value of the Hubbard interaction U_C for which the system undergoes a second order phase transition to a phase with both local FM and AFM order. In the inset of Fig.2 we plot the value of U_C for different values of L and δ_t . Interestingly, all the values of U_C seem to collapse in a unique curve, see Fig.2, when plotted with respect the dimensionless parameter $\bar{\delta}_t = \frac{\delta_t}{\hbar v_F G}$. For small $\bar{\delta}_t$, the critical Hubbard parameter practically coincides with the value $U_C^{AF} = 2.23t_0$ [37, 38] for which pristine graphene undergoes an antiferromagnetic transition. Note however that, in the case of rippled graphene, both FM and AFM local order parameters become finite at the phase transition. For larger values of $\bar{\delta}_t$ the pseudo Landau levels become better defined, the density of states at the Fermi energy increases and therefore U_C drops and eventually, for large enough $\bar{\delta}_t$, becomes zero.

In our numerical calculations we obtain that, for any value of the parameters δ_t , L , and U , the total magnetization of the rippled graphene is zero, in addition and because graphene is a triangular bipartite lattice, the two sublattices have opposite magnetic polarization.

Fig.6 and Fig.7 show the magnetic local order parameters and band structure respectively, for a ripple with $\delta_t = 0.1t_0$, $L = 260a$ and different values of the Hubbard interaction. For this ripple $U_C \sim 0.1t_0$ so that for the values of U plotted in Fig.6 there is always magnetic order. The local FM order appears in the spatial regions $x \sim nL$ and $x \sim n/2 + nL$, where the pseudo effective magnetic fields are larger and the pseudo Landau levels are well defined. The orientation of the spin polarization in these regions is coupled with the orientation of the pseudo magnetic field in such a way that the global FM

order is zero.

This local FM order results in a splitting of the originally degenerated Landau levels and the opening of an energy gap at the Fermi energy, as can be observed in Fig.7. The numerical results indicate that the originally degenerated eight pseudo Landau levels split into two sets of four degenerated pseudo Landau levels, being the occupied states the centered in the region with positive effective magnetic field and spin down that correspond to wavefunctions with amplitude in sublattice A and the centered in the region with negative effective magnetic field and spin up that correspond to wavefunctions with amplitude in sublattice B as schematically shown in Fig. 1 (a).

Superposed to the FM modulation there is an AFM order that for small values of U , is much smaller than the FM order, but that increases with U and for values near U_C^{AF} dominates over the FM order. For these values of U , the self-consistent one-particle Hubbard interaction term in the Hamiltonian is much stronger than the term corresponding to the gauge magnetic fields, and the pseudo Landau levels near zero energy are completely washed out in the band structure, Fig.7. For these large values of U , the relevant parameter is the ratio between U and the tunneling, so that a spatial modulation of the hopping reflects in a modulation of the AFM order. As it is shown in Fig.6, for values of $U \geq U_C^{AF}$ the AFM order parameter is larger in the regions with smaller hopping, $x \sim 3\frac{L}{4} + nL$ and smaller in the regions with larger hopping $x \sim \frac{L}{4} + nL$.

V. SUMMARY

The two-dimensional geometry of graphene makes it unstable against buckling and rippling. In this work we have studied the electric and magnetic properties of rip-

pled graphene. Long wavelength ripples induce a modulation of the hopping parameters in the Hamiltonian of graphene, that translates in the appearance of gauge magnetic fields and pseudo Landau levels. By applying perturbation theory to the modified Dirac equation we have characterized the eight, spin and valley degenerated, zero energy pseudo Landau levels that appears in rippled graphene. For both Dirac cones and spin orientation wavefunction in pseudo Landau levels in regions with positive gauge magnetic field have amplitude only in sublattice A whereas in regions with negative field have weight only on the opposite sublattice B. The high degeneracy at the Fermi energy makes the system prone to interaction instabilities. We have solved self consistently the Hubbard model applied to the tight-binding graphene Hamiltonian and we have found that for moderate values of the Hubbard interaction, the system becomes a gapped quantum Hall local pseudo ferromagnetic state with positive spin polarization in regions with positive effective magnetic field and with the opposite polarization in regions with negative effective gauge field. On top of this local FM order there is an antiferromagnetic order, that increases as U increases and for values of the interaction near U_C^{AF} the system becomes antiferromagnetic with a local order parameter modulated by the amplitude of the hopping. This local pseudo ferromagnetic state, is different from the ground state that will appear in presence of a real magnetic field, and in the mean field Hubbard model is a Néel state.

ACKNOWLEDGMENTS

L.B acknowledges support from MINECO/FEDER under grant FIS2015-64654-P. M.P.L.S. acknowledges financial support by the Spanish MINECO grant FIS2014-57432-P, the European Union structural funds and the Comunidad de Madrid MAD2D-CM Program (S2013/MIT-3007).

-
- [1] P. Avouris, Z. Chen, and V. Perebeinos, *Nat Nano* **2**, 605 (2007).
 - [2] K. S. Novoselov, V. I. Fal[prime]ko, L. Colombo, P. R. Gellert, M. G. Schwab, and K. Kim, *Nature* **490**, 192 (2012).
 - [3] A. H. Castro Neto, F. Guinea, N. M. R. Peres, K. S. Novoselov, and A. K. Geim, *Rev. Mod. Phys.* **81**, 109 (2009).
 - [4] M.I.Katsnelson, *Graphene* (Cambridge, 2012).
 - [5] S. V. Morozov, K. S. Novoselov, M. I. Katsnelson, F. Schedin, L. A. Ponomarenko, D. Jiang, and A. K. Geim, *Physical Review Letters* **97**, 016801 (2006).
 - [6] A. F. Morpurgo and F. Guinea, *Physical Review Letters* **97**, 196804 (2006).
 - [7] J. C. Meyer, A. K. Geim, M. I. Katsnelson, K. S. Novoselov, T. J. Booth, and S. Roth, *Nature* **446**, 60 (2007).
 - [8] F. Guinea, M. I. Katsnelson, and M. A. H. Vozmediano, *Physical Review B* **77**, 075422 (2008).
 - [9] L. Meng, W.-Y. He, H. Zheng, M. Liu, H. Yan, W. Yan, Z.-D. Chu, K. Bai, R.-F. Dou, Y. Zhang, Z. Liu, J.-C. Nie, and L. He, *Physical Review B* **87**, 205405 (2013).
 - [10] K.-K. Bai, Y. Zhou, H. Zheng, L. Meng, H. Peng, Z. Liu, J.-C. Nie, and L. He, *Physical Review Letters* **113**, 086102 (2014).
 - [11] E. Stolyarova, K. T. Rim, S. Ryu, J. Maultzsch, P. Kim, L. E. Brus, T. F. Heinz, M. S. Hybertsen, and G. W. Flynn, *Proceedings of the National Academy of Sciences* **104**, 9209 (2007).
 - [12] M. Ishigami, J. H. Chen, W. G. Cullen, M. S. Fuhrer, and E. D. Williams, *Nano Letters*, *Nano Letters* **7**, 1643 (2007).
 - [13] A. L. Vázquez de Parga, F. Calleja, B. Borca, M. C. G. Passeggi, J. J. Hinarejos, F. Guinea, and R. Miranda,

- Phys. Rev. Lett. **100**, 056807 (2008).
- [14] V. M. Pereira and A. H. Castro Neto, Physical Review Letters **103**, 046801 (2009).
- [15] N. Levy, S. A. Burke, K. L. Meaker, M. Panlasigui, A. Zettl, F. Guinea, A. H. C. Neto, and M. F. Crommie, Science **329**, 544 (2010).
- [16] J. Lu, A. H. C. Neto, and K. P. Loh, Nat Commun **3**, 823 (2012).
- [17] F. Guinea, M. I. Katsnelson, and A. K. Geim, Nat Phys **6**, 30 (2010).
- [18] F. Guinea, A. K. Geim, M. I. Katsnelson, and K. S. Novoselov, Physical Review B **81**, 035408 (2010).
- [19] T. Low and F. Guinea, *Nano Letters*, Nano Letters **10**, 3551 (2010).
- [20] M. Ramezani Masir, D. Moldovan, and F. M. Peeters, *Special Issue: Graphene V: Recent Advances in Studies of Graphene and Graphene analogues*, Solid State Communications **175–176**, 76 (2013).
- [21] B. Roy, F. F. Assaad, and I. F. Herbut, Physical Review X **4**, 021042 (2014).
- [22] G. J. Verbiest, S. Brinker, and C. Stampfer, Physical Review B **92**, 075417 (2015).
- [23] E. Prada, P. San-Jose, G. León, M. M. Fogler, and F. Guinea, Physical Review B **81**, 161402 (2010).
- [24] B. Roy, Z.-X. Hu, and K. Yang, Physical Review B **87**, 121408 (2013).
- [25] S.-Y. Li, K.-K. Bai, L.-J. Yin, J.-B. Qiao, W.-X. Wang, and L. He, Physical Review B **92**, 245302 (2015).
- [26] M. Settnes, N. Leconte, J. E. Barrios-Vargas, A.-P. Jauho, and S. Roche, ArXiv e-prints (2016), arXiv:1607.07300 [cond-mat.mes-hall].
- [27] B. Amorim, A. Cortijo, F. de Juan, A. G. Grushin, F. Guinea, A. Gutiérrez-Rubio, H. Ochoa, V. Parente, R. Roldán, P. San-Jose, J. Schiefele, M. Sturla, and M. A. H. Vozmediano, *Novel effects of strains in graphene and other two dimensional materials*, Physics Reports **617**, 1 (2016).
- [28] E. Tang and L. Fu, Nat Phys **10**, 964 (2014).
- [29] J. W. F. Venderbos and L. Fu, Physical Review B **93**, 195126 (2016).
- [30] B. Tian, M. Endres, and D. Pekker, Physical Review Letters **115**, 236803 (2015).
- [31] J. Sun, H. A. Fertig, and L. Brey, Phys. Rev. Lett. **105**, 156801 (2010).
- [32] K. K. Gomes, W. Mar, W. Ko, F. Guinea, and H. C. Manoharan, Nature **483**, 306 (2012).
- [33] A. D. Zabolotskiy and Y. E. Lozovik, ArXiv e-prints (2016), arXiv:1607.02530 [cond-mat.mes-hall].
- [34] A. Sharma, V. N. Kotov, and A. H. Castro Neto, Physical Review B **87**, 155431 (2013).
- [35] N. M. R. Peres, F. Guinea, and A. H. Castro Neto, Physical Review B **72**, 174406 (2005).
- [36] J. Viana-Gomes, V. M. Pereira, and N. M. R. Peres, Physical Review B **80**, 245436 (2009).
- [37] S. Sorella and E. Tosatti, EPL (Europhysics Letters) **19**, 699 (1992).
- [38] L. M. Martelo, M. Dzierzawa, L. Siffert, and D. Baeriswyl, Zeitschrift für Physik B Condensed Matter **103**, 335 (1996).
- [39] W. A. Harrison, *Electronic Structure and the Properties of Solids* (Dover books on Physics, 1989).
- [40] L. Brey and C. Tejedor, Solid State Communications **48**, 403 (1983).
- [41] L. Brey, C. Tejedor, and J. A. Vergés, Physical Review B **29**, 6840 (1984).
- [42] M. A. H. Vozmediano, M. I. Katsnelson, and F. Guinea, Physics Reports **496**, 109 (2010).
- [43] F. de Juan, M. Sturla, and M. A. H. Vozmediano, Physical Review Letters **108**, 227205 (2012).
- [44] F. de Juan, J. L. Mañes, and M. A. H. Vozmediano, Physical Review B **87**, 165131 (2013).
- [45] We neglect a constant term proportional to τ_x that can be taken away by a gauge transformation.
- [46] M. O. Goerbig, Reviews of Modern Physics **83**, 1193 (2011).
- [47] T. O. Wehling, A. V. Balatsky, A. M. Tsvelik, M. I. Katsnelson, and A. I. Lichtenstein, EPL (Europhysics Letters) **84**, 17003 (2008).
- [48] J. Alicea and M. P. A. Fisher, Physical Review B **74**, 075422 (2006).
- [49] I. F. Herbut, Physical Review B **75**, 165411 (2007).
- [50] V. P. Gusynin, V. A. Miransky, S. G. Sharapov, and I. A. Shovkovy, Physical Review B **74**, 195429 (2006).
- [51] K. Moon, H. Mori, K. Yang, S. M. Girvin, A. H. MacDonald, L. Zheng, D. Yoshioka, and S.-C. Zhang, Physical Review B **51**, 5138 (1995).
- [52] H. A. Fertig, L. Brey, R. Côté, and A. H. MacDonald, Physical Review B **50**, 11018 (1994).
- [53] H. A. Fertig, L. Brey, R. Côté, A. H. MacDonald, A. Karlhede, and S. L. Sondhi, Physical Review B **55**, 10671 (1997).
- [54] H. A. Fertig and L. Brey, Physical Review Letters **97**, 116805 (2006).
- [55] K. Yang, S. Das Sarma, and A. H. MacDonald, Physical Review B **74**, 075423 (2006).
- [56] D. A. Abanin, P. A. Lee, and L. S. Levitov, Physical Review Letters **96**, 176803 (2006).
- [57] M. O. Goerbig, R. Moessner, and B. Douçot, Physical Review B **74**, 161407 (2006).
- [58] K. Yang, *Exploring graphene Recent research advances*, Solid State Communications **143**, 27 (2007).
- [59] S. Das Sarma and K. Yang, Solid State Communications **149**, 1502 (2009).
- [60] J. Jung and A. H. MacDonald, Physical Review B **80**, 235417 (2009).
- [61] Y. Barlas, K. Yang, and A. H. MacDonald, Nanotechnology **23**, 052001 (2012).
- [62] I. L. Aleiner, D. E. Kharzeev, and A. M. Tsvelik, Physical Review B **76**, 195415 (2007).
- [63] M. Kharitonov, Physical Review B **85**, 155439 (2012).